JGR Atmospheres

RESEARCH ARTICLE
10.1029/2023JD038893

Characterization of Thunderstorm Cells Producing Observable Terrestrial Gamma-Ray Flashes

Lasse Skaaning Husbjerg[1], Torsten Neubert[1], Olivier Chanrion[1], Martino Marisaldi[2,3], Martin Stendel[4], Eigil Kaas[4,5], Nikolai Østgaard[2], and Victor Reglero[6]

[1]National Space Institute, Technical University of Denmark (DTU Space), Kgs. Lyngby, Denmark, [2]University of Bergen, Birkeland Centre for Space Science, Bergen, Norway, [3]INAF-OAS Bologna, Bologna, Italy, [4]Danish Meteorological Institute, Copenhagen, Denmark, [5]University of Copenhagen, Niels Bohr Institute, København K, Denmark, [6]Image Processing Laboratory, University of Valencia, Valencia, Spain

Key Points:

- Global analysis of TGF cloud characteristics combining AGILE, ASIM, Fermi and RHESSI
- TGF producing cells are higher than lightning producing cells but otherwise their weather severity is similar
- Regional effects on the meteorological conditions for TGF production are more significant than seasonal effects

Correspondence to:

L. S. Husbjerg,
lhbjrg@space.dtu.dk

Citation:

Husbjerg, L. S., Neubert, T., Chanrion, O., Marisaldi, M., Stendel, M., Kaas, E., et al. (2023). Characterization of thunderstorm cells producing observable Terrestrial Gamma-Ray Flashes. *Journal of Geophysical Research: Atmospheres*, *128*, e2023JD038893. https://doi.org/10.1029/2023JD038893

Received 14 MAR 2023
Accepted 22 AUG 2023

Abstract The meteorological conditions required for the production of Terrestrial Gamma-ray Flashes (TGFs) are not well understood. Particularly, the link between TGF production, meteorology, and weather severity is poorly characterized with most works focusing on only a small set of TGF events or isolated storms. This work is a further step toward understanding the general context of the meteorological conditions required for TGF production and if it differs from regular lightning production. We use TGFs observed from AGILE, ASIM, Fermi, and RHESSI to generate the largest catalog of TGFs with associated lightning sferics from either the World Wide Lightning Location Network (WWLLN) or Global Lightning Detection (GLD) combined with geostationary satellite images and meteorological conditions derived from ERA5 reanalysis data. In total we analyze 1582 TGF events and contextualize them in comparison to lightning flashes as characterized by ASIM. In our analysis we consider the proportion of TGFs and lightning coming from systems with overshooting tops as well as the Cloud Top Temperature (CTT) and the Convective Available Potential Energy (CAPE). Our results are consistent with previous studies, finding that TGFs observed from space come from primarily higher cloud tops than regular lightning flashes do. We find that CAPE and the proportion of cells with overshooting tops is similar for both TGF and lightning producing cells. It suggests that TGF observations from space are biased toward systems with higher cloud tops because the attenuation of the gamma-rays from lower altitude TGFs reduce their intensity below the detection level of LEO instruments.

Plain Language Summary Terrestrial Gamma-ray Flashes (TGFs) are bursts of high energy radiation associated with only some lightning flashes. Here we seek to determine if the systems which generate TGFs are significantly different from those that generate only lightning flashes. While the general trend of TGF observations indicate that observable TGFs come from systems with higher cloud tops than other lightning, relatively little is understood about how the weather severity impacts the production of TGFs. To explore this we use geostationary satellite images and meteorological data to investigate the systems which generate TGFs compared to those that do not. We find that observed TGFs come from systems with higher cloud tops but not significantly more severe weather systems and that regional differences dominate over seasonal differences. It suggests that TGF observations from space are biased toward systems with higher cloud tops, because lower altitude TGFs cannot be detected from the space observatories.

1. Introduction

Terrestrial Gamma-ray Flashes (TGF) are bursts of gamma emissions with an energy range from 100 KeV to 20 Mev and a duration of tens to hundreds of microseconds (Lindanger et al., 2021; Marisaldi et al., 2014). They originate from thunderclouds and differ from other similar events such as leader X-rays due to their higher energy spectrum and generally shorter burst duration (Dwyer et al., 2005). They are thought to be produced due to runaway electron avalanches that lose energy through bremsstrahlung (Bethe et al., 1934; Köhn & Ebert, 2014). Most detections are from space with the major instruments being the Astrorivelatore Gamma ad Immagini LEggero (AGILE) (Marisaldi et al., 2010), Reuven Ramaty High-Energy Spectroscopic Imager (RHESSI) (Grefenstette et al., 2009; Smith et al., 2010), the Fermi Space Telescope (Roberts et al., 2018) and finally the Atmosphere-Space Interactions Monitor (ASIM) (Neubert et al., 2019; Østgaard et al., 2019).

While some studies have focused on the meteorological conditions required for TGFs production, most are either case studies or investigations of single geographic locations (Maiorana et al., 2021; Svechnikova et al., 2020; Tiberia, Mascitelli, et al., 2021; Tiberia, Porcú, et al., 2021; Ursi et al., 2019). Furthermore, the link between weather severity and TGF production is not well understood with TGFs observed from a wide variety of atmospheric conditions (Fabró et al., 2019). These works usually focus on the Convective Available Potential Energy (CAPE) (Fabró et al., 2015), storm extent, Global Convective Diagnostics (GCD) and Cloud Top Height (CTH) (Tiberia et al., 2019; Ursi et al., 2019). Relatively little work exists on large samples of TGFs with geostationary satellites aiding in the analysis. The only recent work is by Ursi et al. (2019), which did not detect significant differences between storms seen to generate TGFs and those that did not.

It is known that TGFs detected from space appear to favor high cloud tops, but whether this is real or just an observational bias is still debated (Chronis et al., 2016). Some studies indicate that an altitude of 15–20 km is required before space based observation platforms can detect TGFs (Dwyer & Smith, 2005). Lower altitude detections of TGFs do exist, particularly during airplane campaigns but observations are rare (Shao et al., 2010; Smith et al., 2016; Xu et al., 2012). Therefore it is an open question whether TGFs favor higher cloud tops and more severe weather or if the detection rate of lower altitude TGFs is simply poor because of the greater atmospheric attenuation of the gamma-rays before reaching the satellites (Chronis et al., 2016; Østgaard et al., 2008).

One way to estimate the weather severity of a thunderstorm or cell is to look for overshooting tops. Overshooting tops are related to powerful deep convection and are an excellent way to gauge weather severity as it requires this deep convection to push the tops of the clouds into the relatively warm lower stratosphere (Bedka, 2011; Marion et al., 2019; Mikuš & Strelec Mahović, 2013). Overshooting tops as a proxy for weather severity in relation to TGFs have so far only been used in case studies (Gjesteland et al., 2015; Maiorana et al., 2021; Smith et al., 2010). In this work we will analyze the proportion of TGFs that come from systems with overshooting tops and compare it to non TGF producing cells as observed by ASIM to determine if TGFs are associated with more severe weather. While previous works did not find differences between storms generating TGFs and those that did not (Ursi et al., 2019), we will focus on the cloud conditions at the time of the TGF.

By combining the four major TGF observing instruments with geostationary satellite data we present the largest TGF meteorology dataset to date. Furthermore, ASIM detected lightning events allows us to compare the TGF producing cells with cells that generate only regular lightning events. Finally, using CAPE and overshooting tops as proxy for convective strength we are able to investigate the weather severity independent of altitude which avoids the known issues of space based TGF observations.

2. Observations and Analysis

2.1. TGF Sample

We seek to determine if there are differences between the TGF producing cells compared to cells which produce only lightning on a global scale. The database of TGFs contains several thousand events from AGILE, ASIM, Fermi, and RHESSI. The instruments used in this work are similar though with some specific differences: AGILE uses 30 independent self-triggering scintillator bars with an energy range of 0.35–100 MeV to look for TGFs and its catalog is based both a cluster and stacking analysis using WWLLN data as input. ASIM detects photons in the range of 20 KeV to >30 Mev using two separate detector modules. One consists of a pixelated Cadmium-Zink-Telluride (CZT) detector crystals low energy detector while the other is a high energy detector of Bismuth-Germanium-Oxide (BGO) modules. ASIM uses the GLD network to associate TGFs with sferics. Fermi consists of 14 scintillator detectors with a range of 8 KeV to 40 MeV and uses the WWLLN network for sferics. Finally, RHESSI has 9 Germanium detectors with a range of 3 KeV to 17 MeV and uses the WWLLN network to associate sferics. Specifics of the thresholds and algorithms to determine TGFs used by each instrument can be found in their respective catalog papers.

However, to investigate the meteorology only TGFs with geolocation from either a WWLLN (World Wide Lightning Location Network) or a Global Lightning Detection (GLD) flash are useable. As such we start from the respective catalogs from each mission. The AGILE data sample contains 1,350 TGFs from March 2015 to December 2021 (Lindanger et al., 2020; Maiorana et al., 2020), ASIM has 536 from June 2018 to December 2020 (Bjørge-Engeland et al., 2022) while Fermi has 1,544 from October 2008 to June 2016 (Roberts et al., 2018) and finally RHESSI has 459 from August 2004 to November 2013 (Lindanger et al., 2022; Smith et al., 2020). The geographic locations of the TGFs used is shown in Figure 1.

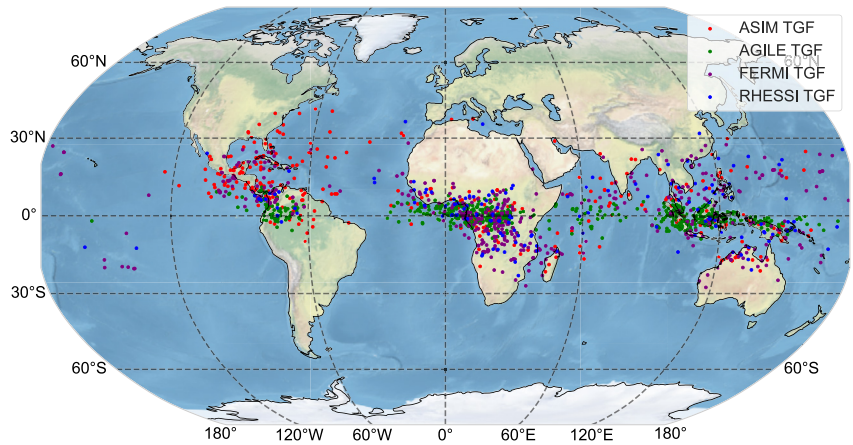

Figure 1. Geographic locations of all TGFs used for this work. Note the difference in higher latitude observations due to orbital differences, particularly noticeable for AGILE and ASIM. A total of 1582 TGFs had both an associated sferic and a geostationary satellite image close in time.

However, as we seek to investigate these TGFs with meteorological conditions derived from geostationary satellite images, associated sferics alone are not enough. We also require that the TGF has an available satellite image within ±15 min of the TGF. While the meteorological conditions can change in 15 min, Ursi et al. (2019) found that their results were not significantly impacted by this time difference and therefore we consider a maximum delay of 15 min to be acceptable. Because of this requirement of a nearby satellite image, the total number of TGFs available for analysis is reduced further. The final sample of TGFs consists of 1,582 events as shown in Table 1. In particular, RHESSI only has 137 from September 2004 to November 2011 because the older geostationary satellites do not often give Full Disk (FD) images.

The latitudinal distribution of the 1,582 TGFs and the lightning comparison dataset are shown in Figure 2. There is a clear connection between the instruments inclination and the latitudes at which they observe TGFs. For this reason it is important to separate high cloud tops from severe weather. Furthermore, each region generating TGFs should be studied separately.

2.2. ASIM Lightning

ASIM detects both lightning and TGFs which makes it the perfect candidate for generating a dataset consisting of lightning producing cells which can be compared to TGF producing cells. On ASIM, it is the Modular Multispectral Imaging Array (MMIA) that detects lightning events (Chanrion et al., 2019). It consists of three photometers which observe in the blue (337 nm), UV (180–235 nm) and red (777.4 nm) allowing it to detect both leader and streamer emissions. Additionally, it has two cameras observing in the same blue and red bands which allow for geolocation of events. Since orbital effects play a role in where TGFs are detected it is ideal to use a platform which can detect both lightning and TGFs to generate the reference dataset. To generate this dataset 20 ASIM detected lightning events per day are chosen from July 2018 to July 2021 and the same parameters gathered as for TGFs. This procedure for choosing lightning events is similar to L. S. Husbjerg et al. (2022), resulting in a total of 8,676 lightning events which have satellite images close in time, available ERA5 and ground based detection from GLD. The latitudinal distribution of these lightning events as seen in Figure 2 is wider than the TGF distributions. This indicates that satellite observed TGFs are likely associated with higher tropopause heights which in turn biases them toward lower latitudes.

Table 1
Statistics of the TGFs Analyzed in the Paper

Instrument	Inclination	Altitude	Total TGFs	TGFs with sferic	TGFs with sferic and satellite image
AGILE	2.47°	509 km	5,344	1,350	679
ASIM	51.64°	413 km	1,254	538	327
Fermi	38.04°	525 km	4,144	1,544	439
RHESSI	25.58°	579 km	2,824	459	137

2.3. Geostationary Satellites

Since the aim is to investigate the global characteristics of TGFs over a long period (2004 to end of 2022) several different geostationary satellites must

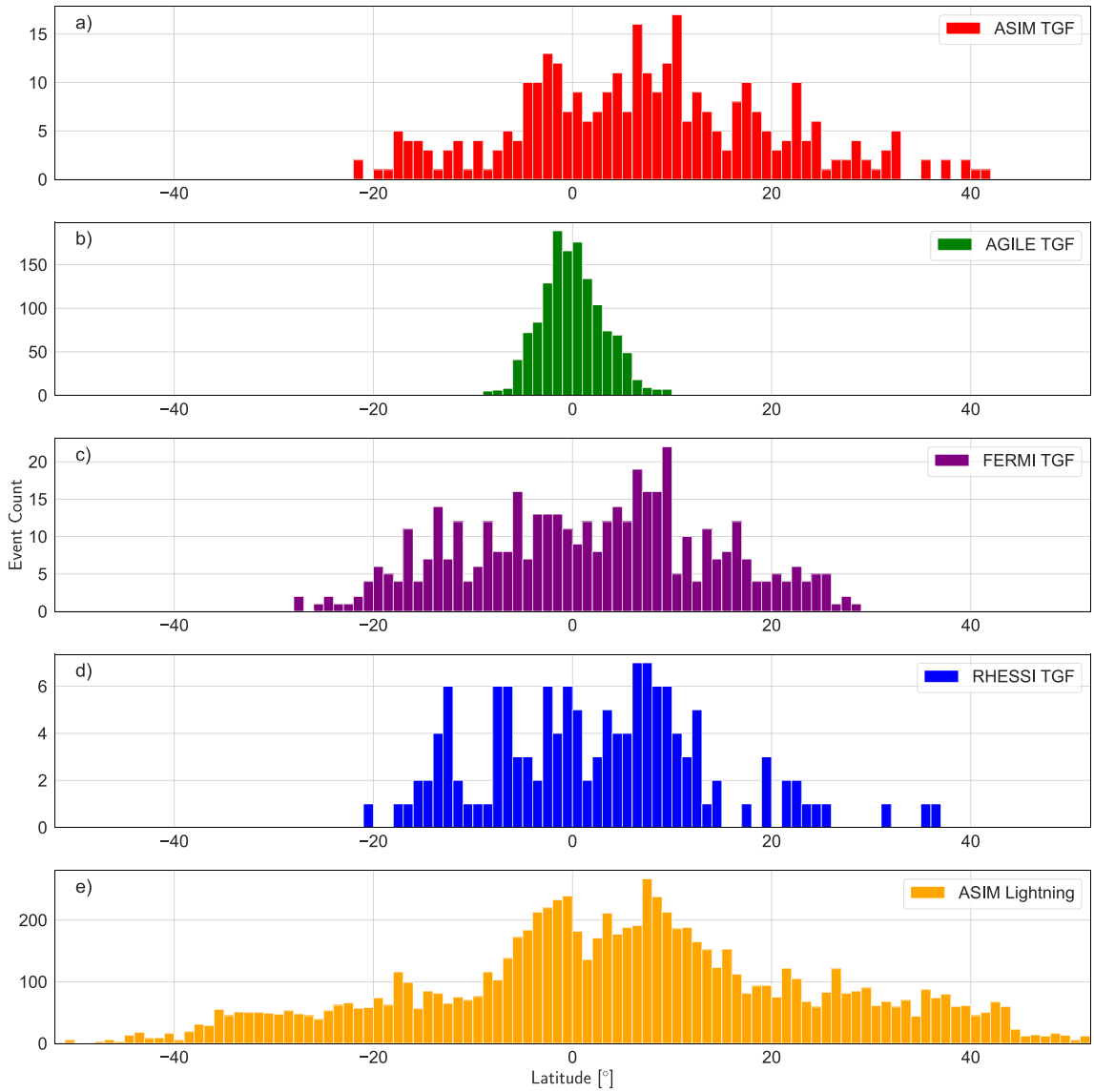

Figure 2. Latitudes of the TGFs and lightning flashes used for the analysis split up by instrument in 1° bins where (a) ASIM, (b) AGILE, (c) FERMI, (d) RHESSI and (e) is the ASIM reference lightning dataset. Each of the observing instruments has a different orbital inclination resulting in different latitudinal distributions. AGILE has the lowest inclination followed by RHESSI, Fermi and finally ASIM with the highest inclination.

be used depending on the location and time of each TGF. Table 2 shows the longitudinal coverage of the geostationary satellites used for the analysis, their spatial resolution and the temporal coverage used for each satellite in this work. In total, 14 different geostationary satellites are used to investigate the events, though we note that for some of the early RHESSI TGFs there is no coverage over South East Asia. The satellites used are: METEOSAT 8–11, FY-2C/D/G, MTSAT-1R/2 and GOES 10–16.

For each of these we gather the Cloud Top Temperature (CTT) from the 10.8 μm band (for some GOES satellites it is 10.7 μm) for each TGF and ASIM detected lightning flash. The location chosen is the coldest pixel within 10 km of the TGF location, considered the average error in the sferic locations from WWLLN and GLD. The same is done for the lightning dataset. While a more advanced definition of cell might be useful when investigating the lifetime of a thunderstorm the focus here is on the instantaneous meteorological conditions of the system producing TGFs.

Table 2
Spatial, Geographic and Temporal Characteristics of the Geostationary Satellites Used for the Analysis

Satellite	Longitude coverage used	Spatial resolution	Temporal coverage used
METEOSAT 8	0 to 70	3 km	After 2016-10-01
FY-2G	70 to 160	5 km	After 2015-06-01
GOES 15	160 to 180 and −180 to −120	4 km	After 2011-01-01
GOES 16	−120 to −30	2 km	After 2018-01-01
METEOSAT 11	−30 to 0	3 km	After 2018-01-01
METEOSAT 10	−30 to 70	3 km	2013-01-01 to 2017-12-1
METEOSAT 9	−30 to 70	3 km	2007-04-01 to 2013-01-01
FY-2D	70 to 160	5 km	2007-08-01 to 2015-06-01
MTSAT-1R	160 to 180	4 km	2005-07-01 to 2010-12-01
GOES 10	−180 to −30	4 km	2004-01-01 to 2009-12-01
GOES 12	−180 to −30	4 km	2010-01-01 to 2013-08-01
GOES 13	−180 to −30	4 km	2009-12-01 to 2018-01-01
METEOSAT 8 (old)	0 to 70	3 km	2004-03-01 to 2007-04-01
FY-2C	70 to 160	5 km	2004-09-01 to 2007-08-01
MTSAT-2	160 to 180	4 km	2010-12-01 to 2015-12-01

2.4. ERA5 Products

ERA5 is the fifth generation of the European Center for Medium-Range Weather Forecasts (ECMWF) reanalysis data set for climate and weather. It contains important estimates of many atmospheric quantities at 1 hr intervals and depending on the parameter it contains data in 137 height levels at $0.25 \times 0.25°$ resolution. For our purposes we need the air temperature to calculate the tropopause temperature and the CAPE to determine the convection. The geostationary satellites provide information about the temperature, and therefore height, of the clouds using the CTT which combined with ERA5 (Hersbach et al., 2023b) can be used to investigate the weather severity. Additionally, we investigate the CAPE at the location of the TGF to see if TGF producing clouds have a higher CAPE than clouds producing only lightning. Given the known connection between CAPE and weather severity this is a reasonable second proxy to determine if TGFs can be said to be correlated with more severe weather than lightning (Murugavel et al., 2014).

A better indication of weather severity than simply CAPE is to investigate the proportion of TGFs coming from systems with overshooting tops. Direct measurements of overshooting tops are difficult. However, they can be estimated using the air temperature available in the ERA5 data. By taking the minimum of the air temperature it is possible to estimate the tropopause temperature and tropopause height at the time and location of the event. If the satellite measured CTT is lower than the tropopause temperature we can deduce that the cloud is in the overshooting phase due to it expanding (and thereby cooling) above the tropopause. Since overshooting tops are strongly related to severe weather this is an excellent proxy for determining if TGFs come from more severe weather than lightning (Borque et al., 2020; Dworak et al., 2012). High clouds by themselves are not necessarily proof of severe weather so it is important to differentiate between strong convection (high CAPE and overshooting tops) and simply high clouds.

3. Results and Discussion

3.1. Global Scale

For the first part of the study, we focus on the CTT of TGFs compared to that of lightning. While it is known that the TGFs observed from space tend to come from high clouds, it is interesting to compare it to the dataset of ASIM detected lightning events as shown in Figure 3 where the events have been grouped into bins of 3 K temperature intervals. We estimated the uncertainty on the quantiles (bins) using the asymptotic normality of the quantiles demonstrated in Serfling (1980) which gives the asymptotic standard deviation for a quantile μ_σ as

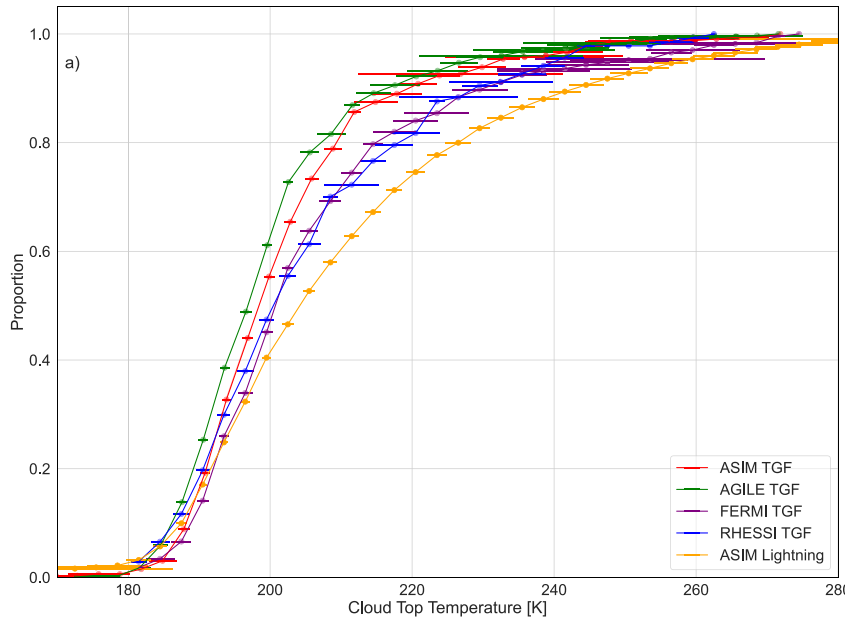

Figure 3. Cumulative distribution of CTT for the observed TGFs compared to that of lightning categorized by the observing instrument. Note the general trend of TGFs occurring in cloud tops colder than those of lightning, indicating that TGFs usually originate from systems with higher cloud tops than lightning.

$\sigma = \frac{\sqrt{\theta(1-\theta)}}{f(\mu_\theta)} \cdot \frac{1}{\sqrt{N}}$ where θ is the Cumulative Distribution Function (CDF), $f(\mu_\theta)$ is the Probability Density Function (PDF) and N is the number of bins. The error bars on Figures 3 and 4 and 6–8 are based on $\pm 1\sigma$ confidence interval. Using this CTT we can then compare the temperatures to the temperature of clouds generating only lightning flashes to see if TGFs occur in higher clouds than that of lightning.

Inspecting Figure 3 shows that TGFs come from cells higher in altitude than regular lightning events. We also see slight differences in the CTT distributions of the observing instruments, particularly we see that RHESSI and Fermi observe a larger fraction of TGFs from systems with higher CTT, indicating a lower altitude than ASIM and AGILE. Due to differences in the orbits and detection efficiency of the observing instruments, it is difficult to be certain that the sample of TGFs analyzed here is truly representative of the general underlying TGF production distribution. However, since the ASIM TGF distribution is largely consistent with those of the other instruments and we use ASIM detected lightning events for the comparison data it strongly indicates that the sample is representative.

Pinpointing the reason why the four instruments do not agree on the distributions of CTT is difficult as each instrument has slightly different detection efficiencies, orbits and use different algorithms to determine if an event is a TGF. However, the most significant reasons are likely related to the difference in the search algorithms combined with differences between ground based networks. Some TGFs with associated sferics are found by looking for TGFs in the instrument and then searching the relevant ground based network for a matching flash while others are found by searching for ground observed flashes and then checking the instrument for a corresponding signal. Additionally, the thresholds of each instrument are different depending on its exact performance which could also result in some differences in the ability to detect weaker TGFs.

These factors can also bias the sample toward different directions, making it difficult to disentangle their contributions. For example, AGILE has a very low inclination orbit, therefore we can expect a bias toward lower CTT values, as observed, being the clouds in the equatorial region higher on average. However, the association to lightning sferics is done based on timing association only, without any additional selection criteria on gamma-ray data. Therefore, even low-significance cluster of counts are selected, possibly associated to lower production altitudes.

The higher altitude of TGF producing cells compared to lightning events may be real or due to observational bias. Therefore we study the weather severity of the cells using two methods, first by investigating the CAPE of the

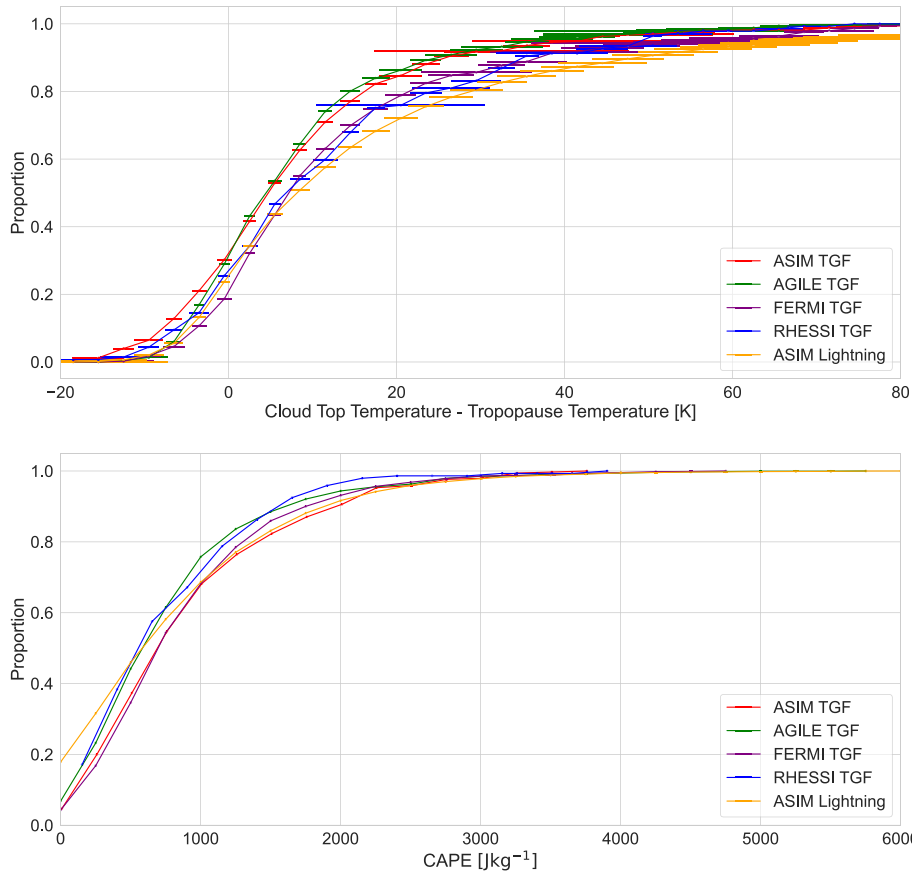

Figure 4. Cumulative distribution for the weather severity parameters for TGFs compared to lightning. (a) Shows the temperature difference between the cloud top and the tropopause where a negative temperature indicates an overshooting top. (b) Shows the CAPE for the TGF producing cells compared to cells generating only lightning. It can be seen that there is no significant difference between the CAPE or proportion of overshooting tops when comparing TGF producing cells to lightning producing cells.

events using ERA5 reanalysis data. Then we further explore the proportion of TGF producing cells which are in the overshooting phase.

In Figure 4 is shown the difference between the CTT and the tropopause temperature where a negative difference indicates that the cell is in the overshooting phase. Unlike Figure 3 which shows a clear difference between the CTTs for TGFs and lightning, when investigating the weather severity there is essentially no observable difference. If we now compare in the case of ASIM observed TGFs and ASIM lightnings to avoid sampling effects due to different observing instruments, we see that there is a barely significant difference. Globally, the number of ASIM observed TGFs coming from systems with overshooting tops is (28 ± 3)% compared to (21 ± 3)% of lightning. This effect is only just significant but has the added benefit of avoiding sampling effects due to different observing instruments.

The CAPE values for TGFs are essentially indistinguishable to those of lightning producing cells. Furthermore the number of TGF producing cells in the overshooting phase is very similar to that of lightning. Given these two results, this is a strong indication that the cells which generate TGFs are not statistically more severe than those which generate only lightning flashes.

So far, the primary comparisons between the observed TGF and lightning distributions have been by comparing the proportion of events above a given threshold such as deep convection or overshooting tops. To formally test if specific data samples appear to come from the same underlying distributions one may run several different tests for significance, the most well known of which is the Kolmogorov-Smirnov (KS) test (Berger & Zhou, 2014). This test essentially uses the largest difference between two CDFs as the test statistic and is therefore easily applicable to the data sets shown. The KS test statistic translates to a *p*-value used to evaluate the significance;

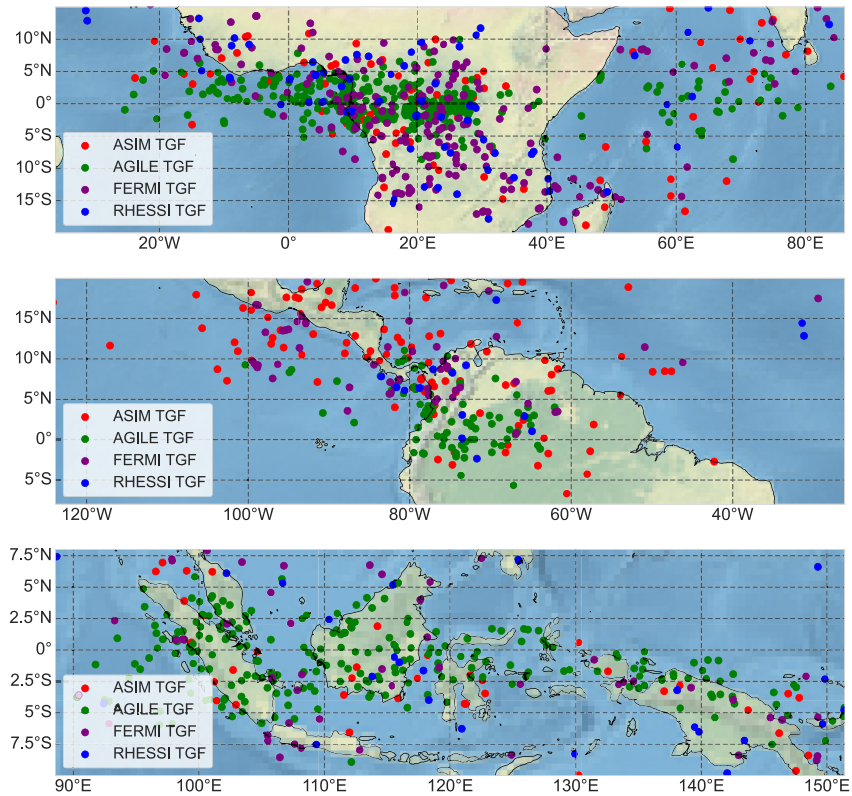

Figure 5. Geographic extent of the regions of particular interest. Central Africa is at the top with South America in the center and South East Asia in the bottom panel.

the test result is considered insignificant (i.e., the distributions are indistinguishable) when p is above a threshold and significant when below. Here we a significance threshold of $p < 0.05$.

Running a two sample KS test with each instrument compared to ASIM lightning for the temperature differences, gives the smallest p-value for the ASIM TGFs with $p = 0.19$ and the largest for FERMI with $p = 0.86$, meaning all comparisons are insignificant. Repeating for the CAPE distributions show that all instruments are again below the significance threshold with RHESSI having the smallest p-value at $p = 0.07$ while ASIM is at $p = 0.24$. FERMI and AGILE are both above $p > 0.90$. These tests confirm that the meteorological distributions for lightning and TGFs appear to be indistinguishable from each other.

Running the KS test on the global CTT distributions rather than the temperature difference distributions show that in this case the tests gives a p-values less than 0.05 for all instruments and are therefore significant showing that in that case lightning and TGF distributions are distinguishable.

Observable TGFs are not more severe than regular lightning flashes but still come from higher cloud tops which may be explained by satellite-based observations being biased toward higher cloud tops. This would explain why the observations show the higher cloud tops for TGFs and also that this effect disappears when measuring weather severity using either CAPE or overshooting tops. This indicates that lower altitude TGFs exist and may be more common than currently known but they remain undetected due to observational bias.

3.2. Regional Scale

It is known that there are three main known regions of TGF production, namely Africa, South America and South East Asia corresponding to the three main lightning chimneys. We investigate each of these regions individually to see how the distributions behave in the regions. Figure 5 shows the geographic extent of the regions with the TGFs detected by each instrument. The largest number of detected TGFs are from Africa, followed by South East Asia and finally South America, which is consistent with lightning production from the three regions.

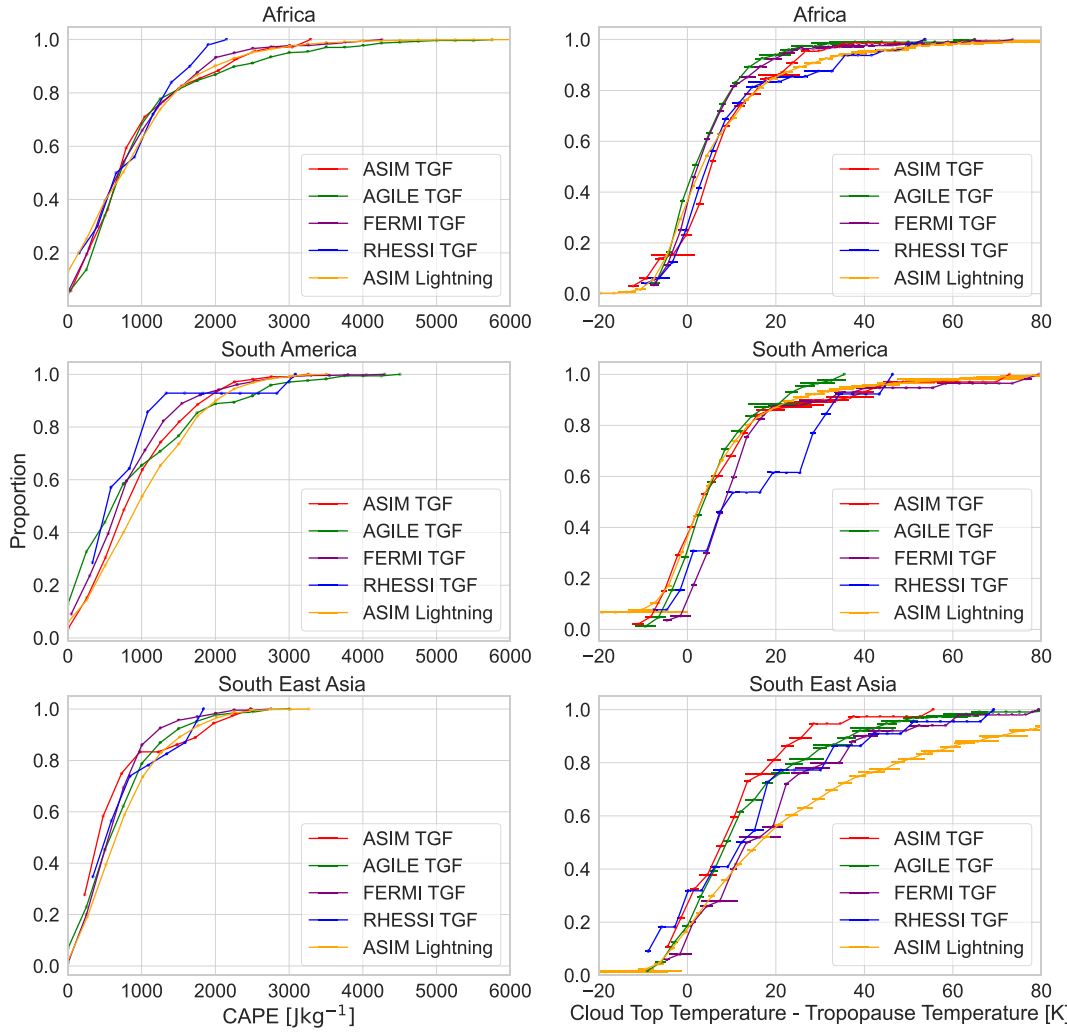

Figure 6. CAPE and temperature differences observed for TGFs in each of the major TGF producing regions. Africa and South America have significantly more TGF events coming from systems with overshooting tops than South East Asia, however they also have significantly more lightning events from systems with overshooting tops.

By splitting the TGF dataset into the major TGF producing regions as mentioned we can now explore the CAPE and temperature difference distributions as seen in Figure 6. It can be seen that the median CAPE is similar for Africa (945 Jkg^{-1}) and South America (925 Jkg^{-1}) while it is slightly smaller for South East Asia (784 Jkg^{-1}). Additionally, the number of events, both lightning and TGF, from deep convection CAPE ≥2,000 Jkg^{-1} for Africa and the Americas are significantly higher than for South East Asia. This shows the known differences in the atmospheric instabilities of the regions. Regardless of these differences the distributions of CAPE for TGFs and lightning remain indistinguishable. From these CAPE distributions we cannot quantitatively see regional differences between the weather severity as characterized by CAPE of TGF producing cells and those that generate only lightning events. It is notable that RHESSI shows higher temperature differences for South America than the other instruments, this is due to the low number of events and available satellite imagery over this region during the time of the RHESSI mission.

Looking again to Figure 6 to see the temperature differences to determine overshooting tops it is clear that for every region that the amount of cells in the overshooting phase is within the uncertainty. As such it would appear that the cells generating TGF events are no more likely to be overshooting the tropopause than any other cell generating lightning in any of the three regions. The temperature differences distributions are indistinguishable for values less than 0. The warmer part of the distributions are different mainly due to the differences in the detection efficiency and orbits of the observing instrument.

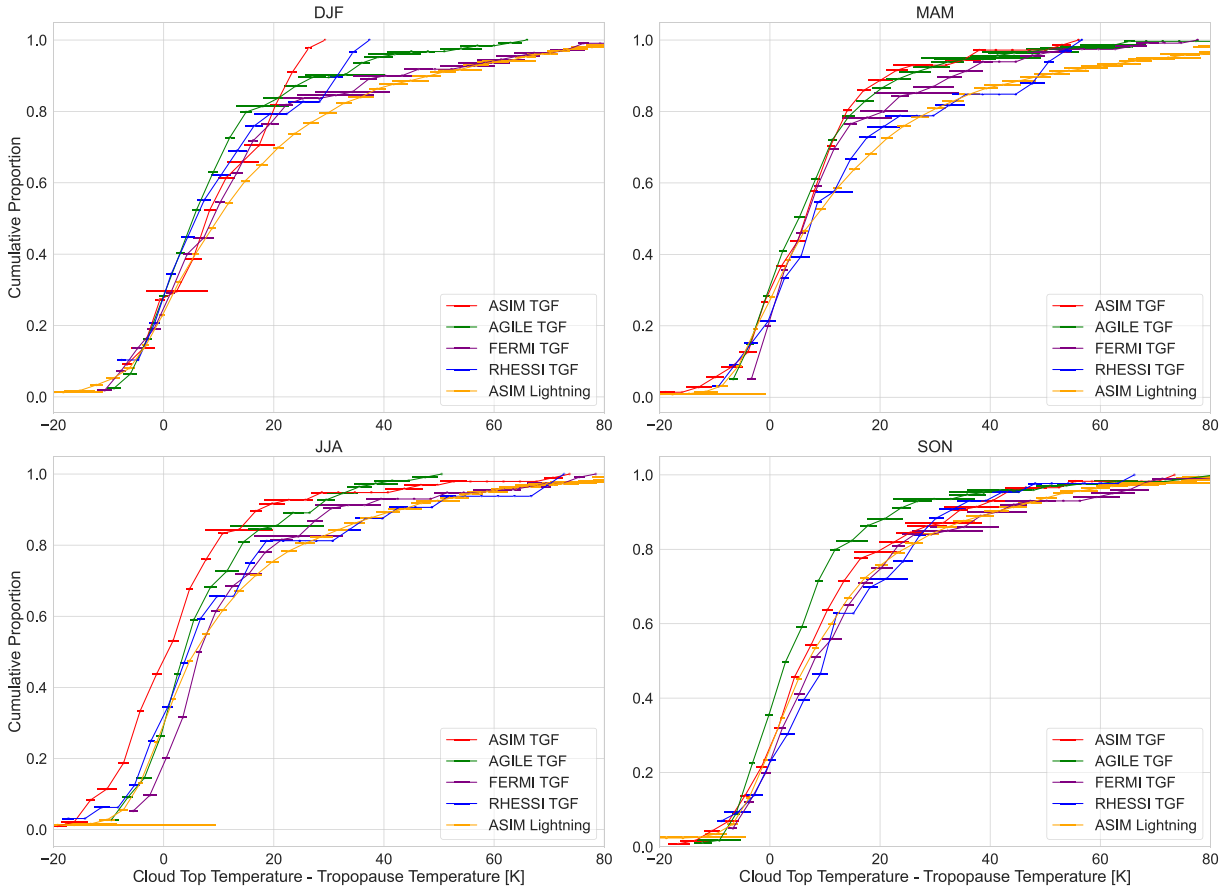

Figure 7. Seasonal temperature differences between the cloud top and the tropopause for TGFs compared to lightning. Each panel shows 3 months. DJF: December, January, February, MAM: March, April, May. JJM: June, July, August. SON: September, October, November.

3.3. Seasonal Scale

We have investigated both the global and local distributions of weather severity and we focus now on the seasonal differences. Figures 7 and 8 show the temperature differences and CAPE values for TGFs compared to lightning for the four seasons. It is noteworthy that there are very little differences between the CAPE distributions, while the temperature differences show that the overshooting tops are again equally likely for TGFs and lightning producing cells. There does not appear to be a systematic difference between them for any season across instruments, only ASIM TGFs appear to show a higher proportion of events coming from systems with overshooting tops for JJA and AGILE TGFs a higher proportion for SON.

The seasonal CAPE distributions follow the expected trend for both TGFs and lightning with lower CAPE values during December to February and highs from June to August. Differences in the CAPE distributions are evident only in the case of AGILE and RHESSI TGFs, specifically during the period spanning June to August. Additionally, there is little difference in the proportion of TGF occurring from systems with overshooting tops as a function of season. This is not entirely unexpected as the tropopause height changes not only with the latitude but also with seasons. Therefore, to get an overshooting top in the local summer requires stronger convection (Appenzeller et al., 1996). However, we do still see more lightning and TGFs from systems with overshooting tops during the more active months from March through August. From this we can see that lightning and TGFs both come from proportionally more severe weather in the months of higher atmospheric instability, but the increase in both are roughly the same. Therefore we do not see any seasonal differences between cells generating lightning and TGFs.

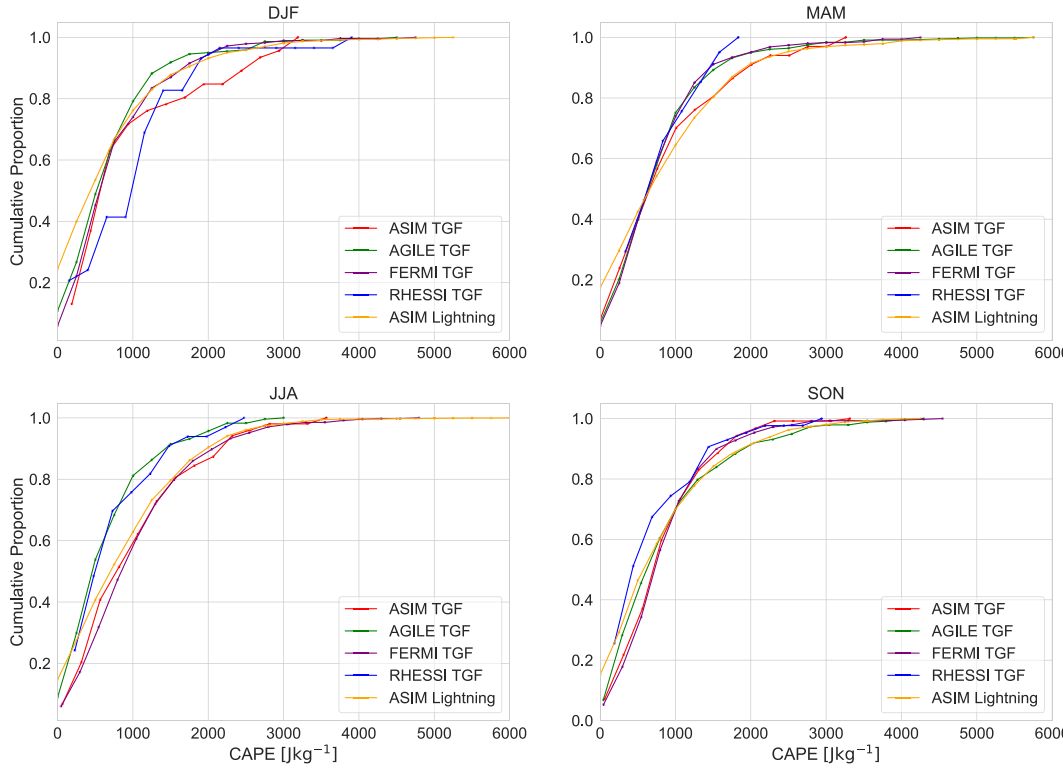

Figure 8. Seasonal CAPE distributions for TGFs compared to lightning. DJF: December, January, February, MAM: March, April, May. JJM: June, July, August. SON: September, October, November.

4. Summary and Conclusions

In this analysis we see that TGF producing cells are mainly found in the low latitude regions. However, the distribution of detected TGFs depends also on the orbit of the observing instrument as shown in earlier works. The TGFs we use have quite a wide distribution of meteorological conditions occurring in many different convective environments including highly severe ones with deep convection but also in weaker and lower cells with low levels of CAPE. This result is consistent with the general consensus that TGFs appear to be generated under a wide variety of convective systems (Chronis et al., 2016; Splitt et al., 2010).

Seasonal effects on the conditions under which TGFs are seen to be generated seem to differ only slightly. While we see significantly more TGFs during the months of the most active lightning producing systems, the conditions under which TGFs are generated do not change. Regional effects however appear to be significant and particularly evident when exploring the differences between the weather severity seen in the African region compared to South East Asia. While Africa has about (30 ± 4)% of TGFs coming from systems with overshooting tops, South East Asia has only (15 ± 2)%. However there is a corresponding difference in the proportion of lightning strokes coming from systems with overshooting tops in each region with Africa having (30 ± 2)% and South East Asia (14 ± 3)%. Results are very similar for the CAPE distributions, with (14 ± 1)% of TGFs occurring in the African region of deep convection CAPE ≥2,000 Jkg^{-1} and (13 ± 1)% of lightning. South East Asia meanwhile has (5 ± 1)% of TGFs occurring during deep convection with (7 ± 1)% of lightning. Due to differences in the observing instruments, the results per instrument change slightly but the general trend is clear: TGFs do not appear to come from systems with overshooting tops or deep convection more often than regular lightning flashes.

This indicates that while there are large differences between the meteorological conditions of various regions, TGFs do not appear to be generated under significantly different conditions compared to lightning. In summary, South East Asia is the region with the least severe weather with (7 ± 1)% of lightning coming from systems in the region of deep convection and (14 ± 2)% from systems with overshooting tops. South America and Africa are similar in terms of weather severity with (16 ± 2)% and (13 ± 1)% of lightning from systems in the region of deep convection respectively. In terms of overshooting tops, South America has (29 ± 5)% of lightning flashes

originating from systems with overshooting tops while Africa has (30 ± 2)%. It is a general trend for the observed TGFs that they come from systems with higher cloud tops than lightning as evidenced by the lower CTT. However because the distributions of TGF and lightning events differ mainly for temperature differences above ≈5 K it appears not to be a result of stronger convection but mainly due to altitude. This strengthens the results found in Maiorana et al. (2021) regarding the lightning/TGF ratio found at mid latitude and points toward observational bias due to atmospheric absorption for low altitude TGFs.

All data here indicates that there is no obvious meteorological difference between the cells which generate TGFs compared to those that produce regular lightning besides the height of the cloud top when observed by Low Earth Orbit (LEO) instruments. The weather severity of the events, when decoupled from altitude indicates that the cells producing TGFs are indistinguishable from those producing only lightning. This is consistent with the idea that the TGFs are mostly detected from high clouds because of the attenuation of gamma-rays by the atmosphere; TGFs from lower clouds have more chances to fall below the detection efficiency of the observing satellite. Additionally, the inability to distinguish systems producing observable TGFs from those producing only lightning indicates that satellite-based observations of TGFs are biased toward higher cloud-top height. It is likely that TGFs are mostly detected from high clouds because of the detection efficiency of LEO instruments and not due to the underlying physical phenomenon.

With this work we complement the current small number of studies analyzing the meteorological conditions related to TGF generation on large catalogs of TGF events and on a larger scale. In particular, more campaigns to detect lower altitude TGFs should be performed to better understand the true underlying altitude distribution of TGFs. Combining aircraft observation with geostationary satellite data would be an excellent way to better probe the meteorological conditions that generate TGF events.

Data Availability Statement

Data supporting this research are available at https://asdc.space.dtu.dk, with agreement from the ASIM Facility Science Team (FST). Interested researchers can submit a research proposal to the FST through asdc@space.dtu.dk. GLD360 data may be obtained through agreement with VAISALA. ERA5 reanalysis data download and instructions are available at Hersbach et al. (2023a, 2023b) for registered users. All satellite images used can be accessed using MCFetch for registered users, with instructions available at https://mcfetch.ssec.wisc.edu/. The RHESSI, Fermi, and AGILE TGF catalogs are available from the following links: https://scipp.pbsci.ucsc.edu/rhessi/, https://fermi.gsfc.nasa.gov/ssc/data/access/gbm/tgf/, and https://www.ssdc.asi.it/mcal3tgfcat/. The data used to generate the figures is available at L. Husbjerg et al. (2023).

Acknowledgments
The authors thank VAISALA for the GLD360 lightning data, ECMWF for the ERA5 reanalysis data and SSEC for making the satellite data available. The authors also wish to thank the World Wide Lightning Location Network (http://wwlln.net), a collaboration among over 50 universities and institutions, for providing the lightning location data used in this paper. The authors thank Ingrid Bjørge Engeland for the ASIM-GLD dataset and Anders Lindanger for the AGILE and RHESSI datasets. ERA5 data was downloaded from the Copernicus Climate Change Service (C3S) Climate Data Store (Hersbach et al., 2023b). The results contain modified Copernicus Climate Change Service information 2020. Neither the European Commission nor ECMWF is responsible for any use that may be made of the Copernicus information or data it contains. The project also received funding from the Independent Research Fund Denmark Grant 1026-00420B. ASIM is a mission of the European Space Agency (ESA) and is funded by ESA and by national grants of Denmark, Norway, and Spain. The ASIM Science Data Centre is supported by ESA PRODEX contracts C 4000115884 (DTU) and 4000123438 (Bergen).

References

Appenzeller, C., Holton, J. R., & Rosenlof, K. H. (1996). Seasonal variation of mass transport across the tropopause. *Journal of Geophysical Research*, *101*(D10), 15071–15078. https://doi.org/10.1029/96JD00821

Bedka, K. M. (2011). Overshooting cloud top detections using MSG SEVIRI Infrared brightness temperatures and their relationship to severe weather over Europe. *Atmospheric Research*, *99*(2), 175–189. https://doi.org/10.1016/j.atmosres.2010.10.001

Berger, V. W., & Zhou, Y. (2014). Kolmogorov–smirnov test: Overview. In *Wiley statsref: Statistics reference online*. John Wiley & Sons, Ltd. https://doi.org/10.1002/9781118445112.stat06558

Bethe, H., Heitler, W., & Dirac, P. A. M. (1934). On the stopping of fast particles and on the creation of positive electrons. *Proceedings of the Royal Society of London - Series A: Containing Papers of a Mathematical and Physical Character*, *146*(856), 83–112. https://doi.org/10.1098/rspa.1934.0140

Bjørge-Engeland, I., Østgaard, N., Mezentsev, A., Skeie, C. A., Sarria, D., Lapierre, J., et al. (2022). Terrestrial gamma-ray flashes with accompanying elves detected by ASIM. *Journal of Geophysical Research: Atmospheres*, *127*(11), e2021JD036368. https://doi.org/10.1029/2021JD036368

Borque, P., Vidal, L., Rugna, M., Lang, T. J., Nicora, M. G., & Nesbitt, S. W. (2020). Distinctive signals in 1-min observations of overshooting tops and lightning activity in a severe supercell thunderstorm. *Journal of Geophysical Research: Atmospheres*, *125*(20), e2020JD032856. https://doi.org/10.1029/2020JD032856

Chanrion, O., Neubert, T., Rasmussen, I. L., Stoltze, C., Tcherniak, D., Jessen, N. C., et al. (2019). The modular multispectral imaging array (MMIA) of the ASIM payload on the international space station. *Space Science Review*, *215*(28), 28. https://doi.org/10.1007/s11214-019-0593-y

Chronis, T., Briggs, M. S., Priftis, G., Connaughton, V., Brundell, J., Holzworth, R., et al. (2016). Characteristics of thunderstorms that produce terrestrial gamma ray flashes. *Bulletin of the American Meteorological Society*, *97*(4), 639–653. https://doi.org/10.1175/BAMS-D-14-00239.1

Dworak, R., Bedka, K., Brunner, J., & Feltz, W. (2012). Comparison between GOES-12 overshooting-top detections, WSR-88D radar reflectivity, and severe storm reports. *Weather and Forecasting*, *27*(3), 684–699. https://doi.org/10.1175/WAF-D-11-00070.1

Dwyer, J. R., Rassoul, H. K., Al-Dayeh, M., Caraway, L., Chrest, A., Wright, B., & Rambo, K. J. (2005). X-ray bursts associated with leader steps in cloud-to-ground lightning. *Geophysical Research Letters*, *32*(1), L01803. https://doi.org/10.1029/2004GL021782

Dwyer, J. R., & Smith, D. M. (2005). A comparison between Monte Carlo simulations of runaway breakdown and terrestrial gamma-ray flash observations. *Geophysical Research Letters*, *32*(22), a–n. https://doi.org/10.1029/2005GL023848

Fabró, F., Montanyà, J., Marisaldi, M., Van der Velde, O. A., & Fuschino, F. (2015). Analysis of global terrestrial gamma ray flashes distribution and special focus on AGILE detections over South America. *Journal of Atmospheric and Solar-Terrestrial Physics*, *124*, 10–20. https://doi.org/10.1016/j.jastp.2015.01.009

Fabró, F., Montanyà, J., Van der Velde, O. A., Pineda, N., & Williams, E. R. (2019). On the TGF/lightning ratio asymmetry. *Journal of Geophysical Research: Atmospheres*, *124*(12), 6518–6531. https://doi.org/10.1029/2018JD030075

Gjesteland, T., Østgaard, N., Laviola, S., Miglietta, M. M., Arnone, E., Marisaldi, M., et al. (2015). Observation of intrinsically bright terrestrial gamma ray flashes from the Mediterranean basin. *Journal of Geophysical Research: Atmospheres*, *120*(23), 12143–12156. https://doi.org/10.1002/2015JD023704

Grefenstette, B. W., Smith, D. M., Hazelton, B. J., & Lopez, L. I. (2009). First RHESSI terrestrial gamma ray flash catalog. *Journal of Geophysical Research*, *114*(A2), a–n. https://doi.org/10.1029/2008JA013721

Hersbach, H. (2023a). ERA5 hourly data on pressure levels from 1940 to present. *Copernicus Climate Change Service (C3S) Climate Data Store (CDS)*. https://doi.org/10.24381/cds.bd0915c6

Hersbach, H. (2023b). ERA5 hourly data on single levels from 1940 to present. *Copernicus Climate Change Service (C3S) Climate Data Store (CDS)*. https://doi.org/10.24381/cds.adbb2d47

Husbjerg, L., Neubert, T., Chanrion, O., Marisaldi, M., Stendel, M., Kaas, E., et al. (2023). Figure data for characterization of thunderstorm cells producing observable terrestrial gamma-ray flashes [Dataset]. Zenodo. https://doi.org/10.5281/zenodo.8032830

Husbjerg, L. S., Neubert, T., Chanrion, O., Dimitriadou, K., Li, D., Stendel, M., et al. (2022). Observations of blue corona discharges in thunderclouds. *Geophysical Research Letters*, *49*(12), e2022GL099064. https://doi.org/10.1029/2022GL099064

Köhn, C., & Ebert, U. (2014). Angular distribution of Bremsstrahlung photons and of positrons for calculations of terrestrial gamma-ray flashes and positron beams. *Atmospheric Research*, *135–136*, 432–465. https://doi.org/10.1016/j.atmosres.2013.03.012

Lindanger, A., Marisaldi, M., Maiorana, C., Sarria, D., Albrechtsen, K., Østgaard, N., et al. (2020). The 3rd AGILE terrestrial gamma ray flash catalog. Part I: Association to lightning Sferics. *Journal of Geophysical Research: Atmospheres*, *125*(11), e2019JD031985. https://doi.org/10.1029/2019JD031985

Lindanger, A., Marisaldi, M., Sarria, D., Østgaard, N., Lehtinen, N., Skeie, C. A., et al. (2021). Spectral analysis of individual terrestrial gamma-ray flashes detected by ASIM. *Journal of Geophysical Research: Atmospheres*, *126*(23), e2021JD035347. https://doi.org/10.1029/2021JD035347

Lindanger, A., Skeie, C. A., Marisaldi, M., Bjørge-Engeland, I., Østgaard, N., Mezentsev, A., et al. (2022). Production of terrestrial gamma-ray flashes during the early stages of lightning flashes. *Journal of Geophysical Research: Atmospheres*, *127*(8), e2021JD036305. https://doi.org/10.1029/2021JD036305

Maiorana, C., Marisaldi, M., Füllekrug, M., Soula, S., Lapierre, J., Mezentsev, A., et al. (2021). Observation of terrestrial gamma-ray flashes at mid latitude. *Journal of Geophysical Research: Atmospheres*, *126*(18), e2020JD034432. https://doi.org/10.1029/2020JD034432

Maiorana, C., Marisaldi, M., Lindanger, A., Østgaard, N., Ursi, A., Sarria, D., et al. (2020). The 3rd agile terrestrial gamma-ray flashes catalog. Part ii: Optimized selection criteria and characteristics of the new sample. *Journal of Geophysical Research: Atmospheres*, *125*(11), e2019JD031986. https://doi.org/10.1029/2019JD031986

Marion, G. R., Trapp, R. J., & Nesbitt, S. W. (2019). Using overshooting top area to discriminate potential for large, intense tornadoes. *Geophysical Research Letters*, *46*(21), 12520–12526. https://doi.org/10.1029/2019GL084099

Marisaldi, M., Fuschino, F., Labanti, C., Galli, M., Longo, F., Del Monte, E., et al. (2010). Detection of terrestrial gamma ray flashes up to 40 MeV by the AGILE satellite. *Journal of Geophysical Research*, *115*(A3). https://doi.org/10.1029/2009JA014502

Marisaldi, M., Fuschino, F., Tavani, M., Dietrich, S., Price, C., Galli, M., et al. (2014). Properties of terrestrial gamma ray flashes detected by AGILE MCAL below 30 MeV. *Journal of Geophysical Research: Space Physics*, *119*(2), 1337–1355. https://doi.org/10.1002/2013JA019301

Mikuš, P., & Strelec Mahović, N. (2013). Satellite-based overshooting top detection methods and an analysis of correlated weather conditions. *Atmospheric Research*, *123*, 268–280. https://doi.org/10.1016/j.atmosres.2012.09.001

Murugavel, P., Pawar, S. D. V., & Gopalakrishan, V. (2014). Climatology of lightning over Indian region and its relationship with convective available potential energy. *International Journal of Climatology*, *34*(11), 3179–3187. https://doi.org/10.1002/joc.3901

Neubert, T., Østgaard, N., Reglero, V., Blanc, E., Chanrion, O., Oxborrow, C. A., et al. (2019). The ASIM mission on the international space station. *Space Science Reviews*, *215*(2), 26. https://doi.org/10.1007/s11214-019-0592-z

Østgaard, N., Balling, J. E., Bjørnsen, T., Brauer, P., Budtz-Jørgensen, C., Bujwan, W., et al. (2019). The modular X- and gamma-ray sensor (MXGS) of the ASIM payload on the international space station. *Space Science Reviews*, *215*(2), e2022GL099064. https://doi.org/10.1007/s11214-018-0573-7

Østgaard, N., Gjesteland, T., Stadsnes, J., Connell, P. H., & Carlson, B. (2008). Production altitude and time delays of the terrestrial gamma flashes: Revisiting the burst and transient source experiment spectra. *Journal of Geophysical Research*, *113*(A2). https://doi.org/10.1029/2007JA012618

Roberts, O. J., Fitzpatrick, G., Stanbro, M., McBreen, S., Briggs, M. S., Holzworth, R. H., et al. (2018). The first fermi-GBM terrestrial gamma ray flash catalog. *Journal of Geophysical Research: Space Physics*, *123*(5), 4381–4401. https://doi.org/10.1029/2017JA024837

Serfling, R. J. (1980). Approximation theorems of mathematical statistics.

Shao, X.-M., Hamlin, T., & Smith, D. M. (2010). A closer examination of terrestrial gamma-ray flash-related lightning processes. *Journal of Geophysical Research*, *115*(A6). https://doi.org/10.1029/2009JA014835

Smith, D. M., Buzbee, P., Kelley, N. A., Infanger, A., Holzworth, R. H., & Dwyer, J. R. (2016). The rarity of terrestrial gamma-ray flashes: 2. RHESSI stacking analysis. *Journal of Geophysical Research: Atmospheres*, *121*(19), 11382–11404. https://doi.org/10.1002/2016JD025395

Smith, D. M., Hazelton, B. J., Grefenstette, B. W., Dwyer, J. R., Holzworth, R. H., & Lay, E. H. (2010). Terrestrial gamma ray flashes correlated to storm phase and tropopause height. *Journal of Geophysical Research*, *115*(A8), a–n. https://doi.org/10.1029/2009JA014853

Smith, D. M., Kelley, N. A., Buzbee, P., Infanger, A., Splitt, M., Holzworth, R. H., & Dwyer, J. R. (2020). Special classes of terrestrial gamma ray flashes from RHESSI. *Journal of Geophysical Research: Atmospheres*, *125*(20), e2020JD033043. https://doi.org/10.1029/2020JD033043

Splitt, M. E., Lazarus, S. M., Barnes, D., Dwyer, J. R., Rassoul, H. K., Smith, D. M., et al. (2010). Thunderstorm characteristics associated with RHESSI identified terrestrial gamma ray flashes. *Journal of Geophysical Research*, *115*(A6). https://doi.org/10.1029/2009JA014622

Svechnikova, E. K., Ilin, N. V., & Mareev, E. A. (2020). Meteorological characteristics of energetic atmospheric phenomena. *Physics of Particles and Nuclei Letters*, *17*(6), 840–847. https://doi.org/10.1134/S1547477120060102

Tiberia, A., Dietrich, S., Porcù, F., Marisaldi, M., Ursi, A., & Tavani, M. (2019). Gamma ray storms: Preliminary meteorological analysis of AGILE TGFs. *Rendiconti Lincei. Scienze Fisiche e Naturali*, *30*(S1), 259–263. https://doi.org/10.1007/s12210-019-00775-y

Tiberia, A., Mascitelli, A., D'Adderio, L. P., Federico, S., Marisaldi, M., Porcù, F., et al. (2021). Time evolution of storms producing terrestrial gamma-ray flashes using era5 reanalysis data, gps, lightning and geostationary satellite observations. *Remote Sensing*, *13*(4), 784. https://doi.org/10.3390/rs13040784

Tiberia, A., Porcú, F., Marisaldi, M., Tavani, M., Lapierre, J., Ursi, A., et al. (2021). GPM-DPR observations on TGFS producing storms. *Journal of Geophysical Research: Atmospheres*, *126*(8), e2020JD033647. https://doi.org/10.1029/2020JD033647

Ursi, A., Marisaldi, M., Dietrich, S., Tavani, M., Tiberia, A., & Porcù, F. (2019). Analysis of thunderstorms producing terrestrial gamma ray flashes with the METEOSAT second generation. *Journal of Geophysical Research: Atmospheres*, *124*(23), 12667–12682. https://doi.org/10.1029/2018JD030149

Xu, W., Celestin, S., & Pasko, V. P. (2012). Source altitudes of terrestrial gamma-ray flashes produced by lightning leaders. *Geophysical Research Letters*, *39*(8). https://doi.org/10.1029/2012GL051351